JACS
JOURNAL OF THE AMERICAN CHEMICAL SOCIETY

COMMUNICATION

pubs.acs.org/JACS

Gadolinium Tagging for High-Precision Measurements of 6 nm Distances in Protein Assemblies by EPR

Hiromasa Yagi,[†] Debamalya Banerjee,[§] Bim Graham,[‡] Thomas Huber,[†] Daniella Goldfarb,*[,§] and Gottfried Otting*[,†]

[†]Research School of Chemistry, Australian National University, Canberra, ACT 0200, Australia

[‡]Medicinal Chemistry and Drug Action, Monash Institute of Pharmaceutical Sciences, Parkville, VIC 3052, Australia

[§]Department of Chemical Physics, Weizmann Institute of Science, Rehovot 76100, Israel

Supporting Information

ABSTRACT: Double electron−electron resonance (DEER) distance measurements of a protein complex tagged with two Gd^{3+} chelates developed for rigid positioning of the metal ion are shown to deliver outstandingly accurate distance measurements in the 6 nm range. The accuracy was assessed by comparison with modeled distance distributions based on the three-dimensional molecular structures of the protein and the tag and further comparison with paramagnetic NMR data. The close agreement between the predicted and experimentally measured distances opens new possibilities for investigating the structure of biomolecular assemblies. As an example, we show that the dimer interface of rat ERp29 in solution is the same as that determined previously for human ERp29 in the single crystal.

Distance measurements on the nanometer scale offer important insights into the long-range structure and conformational changes of biological macromolecules and macromolecular assemblies.[1] As quantitative distance measurements by fluorescence resonance energy transfer are difficult because of the anisotropy of the fluorescent tags, double electron−electron resonance (DEER) experiments have emerged as a powerful alternative tool for measuring distances between unpaired electrons, usually after tagging of the target molecules with nitroxide radicals.[2,3] DEER experiments with gadolinium (Gd^{3+}) tags offer an attractive new approach,[4−7] delivering enhanced sensitivity at higher frequencies (e.g., W-band, 95 GHz) while avoiding the anisotropy effects associated with conformationally restrained nitroxide radicals at W-band frequencies.[5,8] Following conjugation of dipicolinic acid (DPA)−Gd^{3+} tags to proteins by the site-directed spin labeling approach established for nitroxides,[9] distances in the 2.9−3.4 nm range have been measured by W-band DEER.[4,7] Recently, a Gd^{3+}−Gd^{3+} distance of 5.73 nm was measured at the Ka band (∼30 GHz) in a DNA duplex carrying a Gd^{3+} tag at the end of each strand, illustrating the potential for long-range measurements using Gd^{3+} tags.[10] Here we show that through the use of a Gd^{3+}−DOTA amide tag specifically developed for accurate positioning of lanthanide ions (Ln^{3+}),[11] W-band DEER experiments can be employed to measure with outstanding accuracy Gd^{3+}−Gd^{3+} distances of 6 nm in protein assemblies available in subnanomolar amounts. Furthermore, we show that straightforward modeling of the tag conformations with respect to the 3D structure of the protein can reliably predict the Gd^{3+}−Gd^{3+} distances, making the comparison of experimental and predicted distances a most powerful analytical tool. This opens new opportunities for the modeling of large protein assemblies from subunits whose 3D structures are known. We demonstrate the strategy by identifying the dimer interface of the homodimeric rat protein ERp29 in solution.

ERp29 is a chaperone ubiquitously expressed in the endoplasmic reticulum, where it facilitates processing and transport of proteins. Its capacity to assist protein unfolding enhances infection by polyomavirus,[12] and this activity is thought to underpin a role in both carcinogenesis and tumor suppression.[13] The protein forms a 51 kDa homodimer. Dimerization, which is essential for the function, is effected by the N-terminal domain (residues 33 to 150). The C-terminal domain is attached to the N-terminal domain via a flexible peptide segment.[14] The 3D structures of the domains were first determined individually for the rat protein by NMR spectroscopy[14] and subsequently for the full-length human protein by X-ray crystallography.[15] The amino acid sequences of the N-terminal domains of the rat and human proteins are identical except for residue 133 (serine in rat ERp29, threonine in human ERp29). However, different dimer interfaces were identified by NMR spectroscopy and X-ray crystallography. A mutational analysis revealed the double mutant (G37D/D42A) to be compensatory, suggesting that the crystallographically determined interface prevails in solution.[16]

To confirm the dimer interface by a quantitative solution measurement, we reacted the C1 tag loaded with Gd^{3+} (Scheme 1) with single-cysteine mutants of ERp29. The C1 tag is a DOTA amide derivative with a 2-(pyridin-2-yldisulfanyl)ethylacetamide pendant used for spontaneous reaction with a cysteine thiol group to yield a disulfide link.[11] As wild-type ERp29 contains a single cysteine at position 157, new cysteines were introduced at positions 114 and 147 of the ERp29(C157S) mutant. In the following, the double mutants ERp29(S114C/C157S) and ERp29(G147C/C157S) are, for simplicity, called the S114C and G147C mutants, respectively. The S114C mutant was produced as a perdeuterated protein, while the G147C mutant was produced without perdeuteration. Figure 1 shows models of the mutants with tags. The tags were on the external surface of the protein and therefore did not interfere with its native structure. Details of the sample preparation and NMR spectra are

Received: May 13, 2011
Published: June 10, 2011

Scheme 1

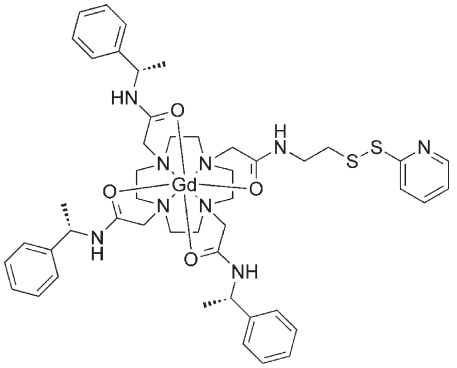

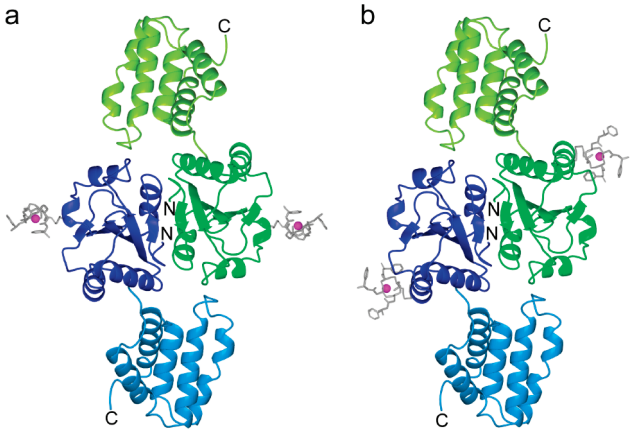

Figure 1. Dimer structure of human ERp29 (PDB ID 2QC7)[15] with the C1−Gd^{3+} tag modeled at (a) position 114 and (b) position 147. The N- and C-termini are labeled. The monomers are shown in blue and green, using darker colors for the N-terminal domain. The tags are drawn in a heavy-atom representation with magenta balls identifying the Gd^{3+} ions.

given in the Figures S1 and S2 in the Supporting Information. The final monomer concentration was 100 μM, with ~90% and ~50% labeling for the S114C and G147C mutants, respectively. Samples were snap frozen for EPR and DEER measurements.

The echo-detected (ED) W-band EPR spectra of the two mutants were similar (Figure S3), comprising a sharp central peak with a width of ~1.1 mT (~30 MHz) from the $|-^1/_2\rangle \rightarrow |^1/_2\rangle$ transition superimposed on a broad background from the other transitions. The narrow and intense central line is a consequence of the high field and the small zero-field splitting arising from the highly symmetric coordination sphere of the Gd^{3+} ion. Figure 2 shows the four-pulse DEER (Figure S4)[17] results for both mutants. The data were recorded with dipolar evolution times (t) as long as 7.5 and 8 μs (see Figures S5 and S6 for data recorded to assess phase memory times and for DEER traces measured under different conditions). Both DEER traces clearly reveal dipolar modulations. Following removal of the background decay, Tikhonov regularization yielded a distance distribution with several peaks, with the most intense peaks at 6.05 and 5.68 nm for the S114C and G147C mutants, respectively. We consider the peaks at shorter distances to be artifacts arising from the noise of the traces, errors in background removal, and incomplete removal of unwanted echoes arising from overlap between the bandwidths

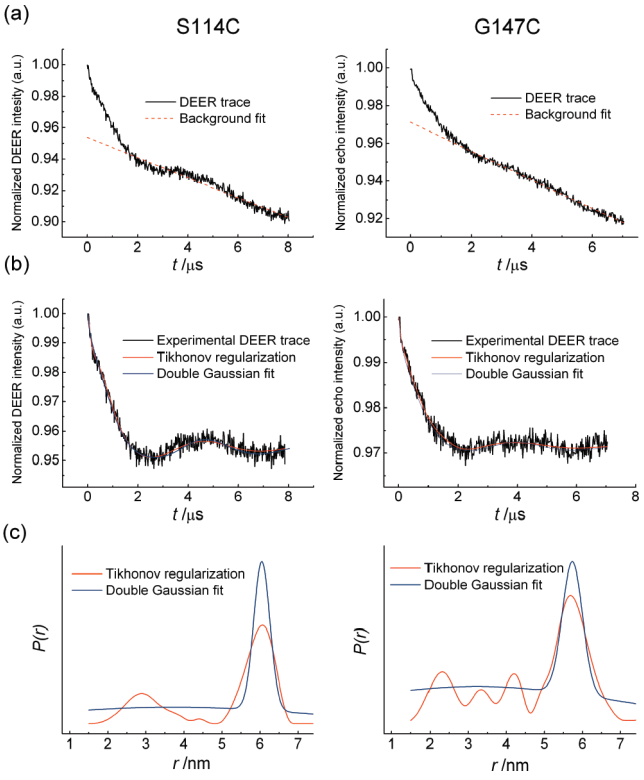

Figure 2. Four-pulse DEER results obtained using ~3 μL of 100 μM frozen solutions of the ERp29 mutants S114C (left) and G147C (right) in 80% D_2O/20% glycerol-d_8 at 10 K. Each spectrum was recorded in ~12 h. (a) Normalized DEER traces fitted with appropriate background decay (in red). (b) Same DEER traces after background removal along with the fits obtained by either Tikhonov regularization (red) or fitting to two Gaussians (blue). (c) Distance distribution obtained by the two different fits shown in (b). The data were analyzed using the program DeerAnalysis.[3] Small dents in the DEER traces at ~4 μs arose from an experimental artifact related to the T interval (Figures S5 and S6).

Table 1. Determination of Distances between Lanthanides Attached to ERp29[a]

	Ln^{3+}−Ln^{3+} distance (nm)		
mutant	DEER	modeling	PCS
S114C	6.05/6.06[b]	6.05	6.02
G147C	5.68/5.74[b]	5.80	5.76

[a] See the main text for details of the distance determinations. [b] Positions of the peak maximum found by Tikhonov regularization (first value) and by a two-Gaussian fit (second value) (see Figure 2).

of the pump and observation pulses (Figure S6). For each mutant, a fit with two Gaussian functions yielded a peak maximum very close to that of the Tikhonov regularization (Figure 2 and Table 1), illustrating the robustness of the distance reported by the main peak, and a broad background accounting for the interferences mentioned above.

To assess the accuracy of the distance measurement afforded by the DEER experiment, we modeled the distance distribution using the crystal structure of the human ERp29 dimer (PDB ID 2QC7)[15] and the crystal structure of the symmetrical parent compound of the C1 tag (DOTAMPh−Gd^{3+} complex, CSD

dx.doi.org/10.1021/ja204415w |J. Am. Chem. Soc. 2011, 133, 10418–10421

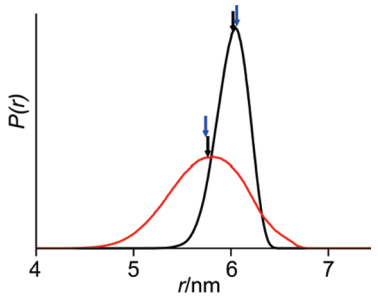

Figure 3. Distributions of the distance between the Gd^{3+} ions in the S114C (black curve) and G147C (red curve) mutants of ERp29 simulated by random variation of the dihedral angles of the tether between the protein and C1 tag. Blue arrows show the distances measured in the DEER experiments (Table 1). Black arrows indicate the distances derived from PCS data by fitting the metal positions and $\Delta\chi$ tensors of Tb^{3+} and Tm^{3+} tags to the crystal structure (PDB ID 2QC7[15]).

accession code EQOZUF).[18] First, the tag was crafted onto single cysteine residues placed at positions 114 and 147. Subsequently, distance distributions between the metals were generated by random variation of the dihedral angles between the C^{α} atom and the amide of the ethylene thio linker of the C1 tag, allowing free rotation around the N−C bond while restricting the sampling to staggered conformations around C−C bonds and dihedral angles of −90° or 90° for the S−S bond with an uncertainty range of ±10°. The protein coordinates were kept fixed, and conformers with steric clashes between tag and protein were eliminated. It was necessary to generate 300 000 (60 000) random conformers for the S114C (G147C) mutant to obtain ∼5000 conformers without steric clashes. To graph the Gd^{3+}−Gd^{3+} distance distributions, the different tag conformers were attached to both protein monomers and all of the pairwise distances (∼2.5×10^7 distances) were calculated. Figure 3 shows the resulting distance distributions.

The maxima of the distance distributions are located remarkably close to those observed by the DEER experiments, suggesting that the DEER measurements delivered the distance between the Gd^{3+} ions with high accuracy (Table 1), although the greater width of the distance distribution for the G147C mutant relative to the S114C mutant (Figure 3) was not reflected in the fit of the experimental DEER data (Figure 2). This excellent agreement lends further strong support to the validity of the DEER data analysis using the standard expressions of two $S = {}^1/_2$ spins[4] and of the DeerAnalysis software.[19]

Because of the bulkiness of the C1 tag, the simulated distance distributions were narrower than those simulated for conventional nitroxide tags such as MTSL.[20] Furthermore, the tag allowed precise distance measurements by unambiguous localization of the electron spin on the Gd^{3+} ion and, most importantly, by its enantiomeric purity, which promotes a single optimal position for the metal ion. In contrast, DOTA tags without defined chirality[10] assume multiple enantiomeric forms[21] that, following attachment to the protein, generate diastereomers with different average metal positions and consequently a larger spread of Gd^{3+}−Gd^{3+} distances in any system with two tags. This effect contributes to the approximately 2-fold narrower distance distributions observed in Figure 2 relative to those reported recently for DNA duplexes with racemic DOTA−Gd^{3+} tags.[10]

To obtain an independent assessment of the dimer, we attached C1 tags loaded with Tb^{3+}, Tm^{3+}, and Y^{3+} to uniformly ^{15}N-labeled and selectively ^{15}N-Lys labeled samples of the S114C and G147C mutants and measured pseudocontact shifts (PCSs) of amide protons in ^{15}N HSQC spectra. The PCSs were measured as the differences in chemical shifts observed with paramagnetic (Tb^{3+}, Tm^{3+}) and diamagnetic (Y^{3+}) metal ions (Figure S1). The PCSs were used to fit magnetic susceptibility anisotropy ($\Delta\chi$) tensors to each conformer of the generated ensembles in order to simulate the Gd^{3+}−Gd^{3+} distance distributions of Figure 3. Fits with the smallest residual deviations between experimental and back-calculated PCSs were deemed acceptable if the sum of squared deviations (ΔX^2) was less than 1.1 times that of the best fit (ΔX^2_{best}).

The best fits were in excellent agreement with the experimental PCSs (Figure S2), confirming the tag attachment sites and the Gd^{3+}−Gd^{3+} distances measured using DEER (Table 1). Accepting fits with $\Delta X^2 < 1.1\Delta X^2_{best}$ produced a distribution of Ln^{3+}−Ln^{3+} distances (5.90−6.35 nm for the S114C mutant and 5.65−6.09 nm for the G147C mutant). The averages of those distributions (6.08 and 5.86 nm, respectively) were within 0.1 nm of the distances of the best fits (Table 1) and within 0.2 nm of the distance distribution maxima measured using DEER.

The PCSs also provided evidence for the dimer interface of the crystal structure[15] by yielding smaller ΔX^2_{best} values for the dimer than for the monomer (Figure S2). However, the difference in fitting quality was quite small, which may be attributed to the large number of parameters that had to be fitted [axial and rhombic components of the $\Delta\chi$ tensor, the (x, y, z) coordinates of the metal ion, and three Euler angles] and the large distance of the Ln^{3+} ions from the dimer interface (Figure 1).

In summary, the close agreement of the DEER and NMR data with the crystal structure of human ERp29 unequivocally confirms that the dimer interface of the crystal structure prevails in solution. This result supersedes the very different dimer interface proposed on the basis of the earlier NMR results, for which the distance between the Ser114 C^{β} atoms across the dimer interface would have been less than 2 nm. The earlier proposal relied on protection from proton exchange with the solvent and on accessibility to the paramagnetic agent Gd(DTPA-BMA).[14] It appears that although the NMR structure delivered the correct overall protein fold, its accuracy was insufficient to interpret structural details such as the solvent exposure of some of the amides. In addition, paramagnetic relaxation enhancements were misinterpreted (which may be attributed to the limited sensitivity and resolution of the ^{15}N TROSY spectra and inaccuracies in the NMR structure), although it was noted that the amide of Gly92 unexpectedly seemed to be protected[14] (its protection is predicted by the crystallographic dimer interface). By confirming the crystallographically determined dimer interface of ERp29 in solution, the present data also indicate that by virtue of its similarity to ERp29, the crystallographically determined interface of the *Drosophila* homologue Wind is maintained in solution.[22]

Measurement of Gd^{3+}−Gd^{3+} distances greater than 6 nm may be possible with additional optimizations. Compared to tags derived from DPA,[23] the much higher Gd^{3+} binding affinity of DOTA-based tags eliminates unbound Gd^{3+} ions that otherwise would contribute to the background in DEER experiments. This and the narrower central line may explain why the modulation depths of the DEER traces in Figure 2b are significantly greater than in our previous experiments with DPA tags.[5] In addition, a highly saturated coordination sphere avoids complications from undesired intermolecular interactions.[7] Interestingly, the phase memory time (T_M) of the perdeuterated S114C mutant was not

much longer than that of the undeuterated G147C mutant, whereas in the case of MTSL-labeled proteins, perdeuteration of the protein has been shown to extend the T_M of nitroxide radicals substantially, allowing a maximum dipolar evolution time of 25 μs.[24] On the basis of the T_M value of the perdeuterated S114C mutant, the dipolar evolution time could be extended to 10 μs, affording distance measurements up to 8 nm.[3] Measurements of even longer Gd^{3+}−Gd^{3+} distances may be facilitated more significantly by perdeuteration of the C1 tag or by instrumentation that allows measurements of larger volumes of sample at lower concentrations.[25] Increased sensitivity may also result from narrower distance distributions obtained by immobilizing DOTA-type Gd^{3+} complexes by two-armed attachment.[26] For sterically demanding tagging sites, a smaller, chiral DOTA derivative may be equally suitable.[27]

In conclusion, the isotropic nature of the Gd^{3+} ion spectrum lends itself to extraordinarily accurate nanometer-scale distance measurements using high-field DEER experiments on samples containing 0.2−0.3 nmol of protein. Combined with the possibility of accurate prediction of the distances by modeling, this presents an outstanding tool for establishing the structure and conformation of biological macromolecular assemblies in a small number of experiments.

■ ASSOCIATED CONTENT

Supporting Information. Descriptions of sample preparations and NMR and EPR experiments; NMR spectra and tables of PCSs and fitted $\Delta\chi$ tensors; correlation of back-calculated and experimental PCSs; echo-detected EPR spectrum; plot of echo intensity versus echo delay; and raw DEER traces. This material is available free of charge via the Internet at http://pubs.acs.org.

■ AUTHOR INFORMATION

Corresponding Author
daniella.goldfarb@weizmann.ac.il; gottfried.otting@anu.edu.au

■ ACKNOWLEDGMENT

We thank Dr. Souren Mkrtchian for the expression vector of ERp29. Financial support by the Australian Research Council, including a Future Fellowship to T.H., and by the Binational Science Foundation (USA−Israel, BSF#2006179 to D.G.) is gratefully acknowledged. D.G. holds the Erich Klieger Professorial Chair in Chemical Physics.

■ REFERENCES

(1) (a) Altenbach, C.; Kusnetzow, A. K.; Ernst, O. P.; Hofmann, K. P.; Hubbell, W. L. *Proc. Natl. Acad. Sci. U.S.A.* **2008**, *105*, 7439. (b) Borbat, P. P.; Mchaourab, H. S.; Freed, J. H. *J. Am. Chem. Soc.* **2002**, *124*, 5304. (c) Dockter, C.; Volkov, A.; Bauer, C.; Polyhach, Y.; Joly-Lopez, Z.; Jeschke, G.; Paulsen, H. *Proc. Natl. Acad. Sci. U.S.A.* **2009**, *106*, 18485. (d) Yang, Y.; Ramelot, T. A.; McCarrick, R. M.; Ni, S.; Feldmann, E. A.; Cort, J. R.; Wang, H.; Ciccosanti, C.; Jiang, M.; Janjua, H.; Acton, T. B.; Xiao, R.; Everett, J. K.; Montelione, G. T.; Kennedy, M. A. *J. Am. Chem. Soc.* **2010**, *132*, 11910.

(2) (a) Fanucci, G. E.; Cafiso, D. S. *Curr. Opin. Struct. Biol.* **2006**, *16*, 644. (b) Schiemann, O.; Prisner, T. F. *Q. Rev. Biophys.* **2007**, *40*, 1. (c) Borbat, P. P.; Freed, J. H. *Methods Enzymol.* **2007**, *423*, 117. (d) Reginsson, G. W.; Schiemann, O. *Biochem. J.* **2011**, *434*, 353.

(3) Jeschke, G.; Polyhach, Y. *Phys. Chem. Chem. Phys.* **2007**, *9*, 1895.

(4) Potapov, A.; Song, Y.; Meade, T. J.; Goldfarb, D.; Astashkin, A. V.; Raitsimring, A. *J. Magn. Reson.* **2010**, *205*, 38.

(5) Potapov, A.; Yagi, H.; Huber, T.; Jergic, S.; Dixon, N. E.; Otting, G.; Goldfarb, D. *J. Am. Chem. Soc.* **2010**, *132*, 9040.

(6) Raitsimring, A. M.; Gunanathan, C.; Potapov, A.; Potapov, A.; Efremenko, I.; Martin, J. M. L.; Milstein, D.; Goldfarb, D. *J. Am. Chem. Soc.* **2007**, *129*, 14138.

(7) Gordon-Grossman, M.; Kaminker, I.; Goldfarb, D. *Phys. Chem. Chem. Phys.* **2011**, *13*, 10771.

(8) Polyhach, Y.; Godt, A.; Bauer, C.; Jeschke, G. *J. Magn. Reson.* **2007**, *185*, 118.

(9) Hubbell, W. L.; Gross, A.; Langen, R.; Lietzow, M. A. *Curr. Opin. Struct. Biol.* **1998**, *8*, 649.

(10) Song, Y.; Meade, T. J.; Astashkin, A. V.; Klein, E. L.; Enemark, J. H.; Raitsimring, A. *J. Magn. Reson.* **2011**, *148*, 379.

(11) Graham, B.; Loh, C. T.; Swarbrick, J. D.; Ung, P.; Shin, J.; Yagi, H.; Jia, X.; Chhabra, S.; Pintacuda, G.; Huber, T.; Otting, G. *Bioconjugate Chem.*, submitted.

(12) Rainey-Barger, E. K.; Mkrtchian, S.; Tsai, B. *J. Virol.* **2009**, *83*, 1483.

(13) Zhang, D.; Richardson, D. R. *Int. J. Biochem. Cell Biol.* **2011**, *43*, 33.

(14) Liepinsh, E.; Baryshev, M.; Sharipo, A.; Ingelman-Sundberg, M.; Otting, G.; Mkrtchian, S. *Structure* **2001**, *9*, 457.

(15) Barak, N. N.; Neumann, P.; Sevvana, M.; Schutkowski, M.; Naumann, K.; Malesevic, M.; Reichart, H.; Fischer, G.; Stubbs, M. T.; Ferrari, D. M. *J. Mol. Biol.* **2009**, *385*, 1630.

(16) Rainey-Barger, E. K.; Mkrtchian, S.; Tsai, B. *Mol. Biol. Cell* **2007**, *18*, 1253.

(17) Pannier, M.; Veit, S.; Godt, A.; Jeschke, G.; Spiess, H. W. *J. Magn. Reson.* **2000**, *142*, 331.

(18) Parker, D.; Puschmann, H.; Batsanov, A. S.; Senanayake, K. *Inorg. Chem.* **2003**, *42*, 8646.

(19) Jeschke, G.; Chechik, V.; Ionita, P.; Godt, A.; Zimmermann, H.; Banham, J.; Timmel, C. R.; Hilger, D.; Jung, H. *Appl. Magn. Reson.* **2006**, *30*, 473.

(20) Polyhach, Y.; Bordignon, E.; Jeschke, G. *Phys. Chem. Chem. Phys.* **2011**, *13*, 2356.

(21) Parker, D.; Dickins, R. S.; Puschmann, H.; Crossland, C.; Howard, J. A. K. *Chem. Rev.* **2002**, *102*, 1977.

(22) Ma, Q.; Guo, C.; Barnewitz, K.; Sheldrick, G. M.; Söling, H.-D.; Usón, I.; Ferrari, D. M. *J. Biol. Chem.* **2003**, *278*, 44600.

(23) (a) Su, X.-C.; Man, B.; Beeren, S.; Liang, H.; Simonsen, S.; Schmitz, C.; Huber, T.; Messerle, B. A.; Otting, G. *J. Am. Chem. Soc.* **2008**, *130*, 10486. (b) Man, B.; Su, X.-C.; Liang, H.; Simonsen, S.; Huber, T.; Messerle, B. A.; Otting, G. *Chem.—Eur. J.* **2010**, *16*, 3827. (c) Jia, X.; Maleckis, A.; Huber, T.; Otting, G. *Chem.—Eur. J.* **2011**, *17*, 6830.

(24) Ward, R.; Bowman, A.; Sozudogru, E.; El-Mkami, H.; Owen-Hughes, T.; Norman, D. G. *J. Magn. Reson.* **2010**, *207*, 164.

(25) Cruickshank, P. A.; Bolton, D. R.; Robertson, D. A.; Hunter, R. I.; Wylde, R. J.; Smith, G. M. *Rev. Sci. Instrum.* **2009**, *80*, No. 103102.

(26) (a) Vlasie, M. D.; Comuzzi, C.; van den Nieuwendijk, A. M.; Prudêncio, M.; Overhand, M.; Ubbink, M. *Chem.—Eur. J.* **2007**, *13*, 1715. (b) Keizers, P. H.; Desreux, J. F.; Overhand, M.; Ubbink, M. *J. Am. Chem. Soc.* **2007**, *129*, 9292.

(27) Häussinger, D.; Huang, J. R.; Grzesiek, S. *J. Am. Chem. Soc.* **2009**, *131*, 14761.